

# A Thermally Stable {FeNO}<sup>8</sup> Complex: Properties and Biological Reactivity of Reduced MNO Systems

Ashis K. Patra,<sup>a</sup> Koustubh S. Dube,<sup>a</sup> Brian C. Sanders,<sup>a</sup> Georgia C. Papaefthymiou,<sup>b</sup> Jeanet Conradie,<sup>c,d</sup> Abhik Ghosh,<sup>d</sup> and Todd C. Harrop<sup>\*a</sup>

5

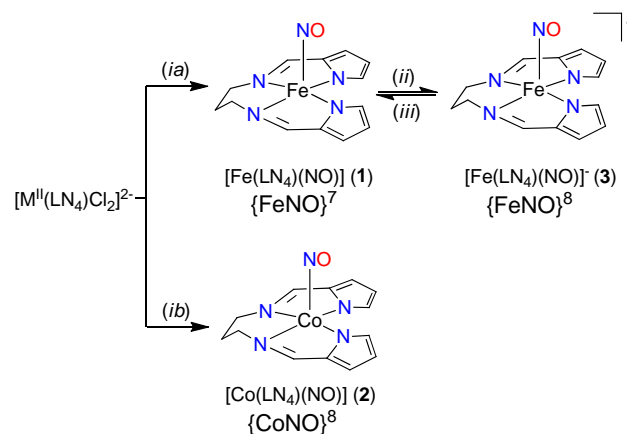
Reduced nitrogen oxide ligands such as NO<sup>-</sup>/HNO or nitroxyl participate in chemistry distinct from nitric oxide (NO). Nitroxyl has been proposed to form at heme centers to generate the Enemark-Feltham designated {FeNO}<sup>8</sup> system. The synthesis of a thermally stable {FeNO}<sup>8</sup> species namely,  
10 [Co(Cp\*)<sub>2</sub>][Fe(LN<sub>4</sub>)(NO)] (**3**), housed in a heme-like ligand platform has been achieved by reduction of the corresponding {FeNO}<sup>7</sup> complex, [Fe(LN<sub>4</sub>)(NO)] (**1**), with decamethylcobaltocene [Co(Cp\*)<sub>2</sub>] in toluene. This complex readily reacts with metMb resulting in formation of MbNO via reductive nitrosylation by the coordinated HNO/NO<sup>-</sup>, which can be inhibited with GSH. These results suggest **3** could serve as a potential HNO therapeutic. The spectroscopic, theoretical, and structural comparisons are  
15 made to **1** and the {CoNO}<sup>8</sup> complex, [Co(LN<sub>4</sub>)(NO)] (**2**), an isoelectronic analogue of **3**.

## Introduction

The one-electron reduced form of nitric oxide (NO), namely NO<sup>-</sup>/HNO or nitroxyl (pK<sub>a</sub> = 11.4), has been shown to engage in biologically relevant chemistry distinct from NO.<sup>1-3</sup> For example,  
20 HNO donors have been used as anti-alcoholism agents<sup>2a</sup> and are proving to be promising therapeutics against heart failure.<sup>2b-d</sup> Like NO, nitroxyl has been proposed to be generated and targeted at a variety of heme-containing proteins.<sup>3</sup> Indeed, transient iron-nitroxyl intermediates have been suggested in the catalytic cycles  
25 of heme proteins involved in biological denitrification like nitrite reductase (NiR), NO reductase (NOR)<sup>3a,4</sup> and at NO synthase (NOS) under certain conditions.<sup>1a</sup> Accordingly, these nitroxyl-bound species are classified according to the Enemark-Feltham notation as {FeNO}<sup>8</sup> systems.<sup>5</sup> In addition to these biological  
30 examples, small-molecule derivatives of iron-porphyrins (Fe-por),<sup>6</sup> a non-heme Fe-cyclam complex,<sup>7</sup> and nitroprusside<sup>8</sup> have produced {FeNO}<sup>8</sup> systems. The reactivity of these few {FeNO}<sup>8</sup> complexes has never been explored and most are only characterized by *in situ* spectroscopy/electrochemistry where a  
35 discrete complex has not been isolated. Thus, there remains a lack of spectroscopic in combination with reactivity data to aid in the identification of the elusive {FeNO}<sup>8</sup> intermediate. Studies on small molecules; however, will establish the foundation to identify and ultimately predict the fate of such species traversed  
40 in biology as demonstrated in a {CuNO}<sup>10</sup> NiR model.<sup>9</sup> The lack of benchmarks for the {FeNO}<sup>8</sup> formalism highlights the need for such systems to be constructed. Herein, we present the synthesis, structure, and spectroscopic/theoretical properties of discrete {MNO}<sup>7/8</sup> complexes (where M = Fe, Co) and report  
45 their reactivity with ferric myoglobin (metMb) and glutathione (GSH).

## Results and Discussion

The LN<sub>4</sub> ligand (Scheme 1) was designed and utilized in this work as a simple non-macrocylic heme platform. Reaction of  
50 NO(g) with the Fe(II) complex, (Et<sub>4</sub>N)<sub>2</sub>[Fe(LN<sub>4</sub>)Cl<sub>2</sub>], in MeCN at room temperature (RT) generated the green microcrystalline {FeNO}<sup>7</sup> complex, [Fe(LN<sub>4</sub>)(NO)] (**1**), in 79% yield (Scheme 1). The analogous Co species was synthesized similarly affording the dark-red {CoNO}<sup>8</sup> complex, [Co(LN<sub>4</sub>)(NO)] (**2**), in 75% yield.  
55 Complexes **1** and **2** appear stable – no dissociation or reaction of the coordinated NO was observed with excess gas (NO, O<sub>2</sub>) purge, vacuum or ordinary laboratory light.<sup>10</sup>



**Scheme 1** Synthetic Route Towards {MNO}<sup>7/8</sup> Complexes (ia, M = Fe; ib, M = Co) NO(g), MeCN, RT; (ii) [Co(Cp\*)<sub>2</sub>], toluene, RT; (iii) [Fe(Cp\*)<sub>2</sub>][PF<sub>6</sub>], MeCN, RT.

X-ray structures revealed five-coordinate (5C) square-pyramidal (Sq-Py) coordination modes for the metal centers in **1**

and **2** (Fig. 1). The structure of **1** exhibits two distinct but similar molecules in the unit cell (see the ESI†). The Fe center in **1** is in a distorted Sq-Py ( $\tau_{\text{avg}} = 0.31$ ) originating from the four basal N-ligands of  $[\text{LN}_4]^{2-}$  that are asymmetrically coordinated and one quasi-linear-to-slightly bent NO (Fig. 1). Complex **1** is a rare example of an  $\{\text{FeNO}\}^7$  complex that exhibits an average Fe–N–O angle of  $\sim 160^\circ$ ,<sup>11</sup> significantly above the normal range of 140–145°.<sup>12</sup> The quasi-linear nature of this bond angle has been ascribed to significant metal  $d_{z^2}$ - $p_z$  mixing, which minimizes repulsion between the Fe  $d_{z^2}$  and the  $\sigma$  lone-pair of NO.<sup>11d</sup> In contrast, the average N–O distance in **1** (1.171 Å) is more typical (1.15–1.18 Å).<sup>12</sup> Analogous to Fe-por-NO species, the Fe center in **1** is displaced out of the  $\text{N}_4$  plane, and towards NO, by 0.46 Å. Such out-of-plane deviations toward NO are also observed in other  $\{\text{FeNO}\}^7$  porphyrin complexes.<sup>ref</sup> Crystals of **2** revealed a similar geometry about Co much like **1** ( $\tau = 0.27$ ) (Fig. 1). The N–O distance of 1.1551(15) Å in **2** is shorter compared to **1**. This difference is further reflected in the M–NO distance, which is longer in **2** (1.7890(11) Å) than **1** (avg: 1.6994(12) Å) suggesting potential lability of the M–NO bond in  $\{\text{MNO}\}^8$  systems. The severely bent Co–N–O angle (125.97°) is characteristic of  $\{\text{CoNO}\}^8$  type complexes.<sup>12,13</sup>

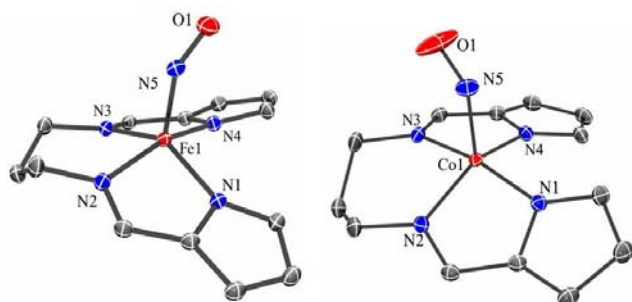


**Fig. 1** ORTEP diagrams of  $[\text{Fe}(\text{LN}_4)(\text{NO})]$  (**1**) (one unique molecule) and  $[\text{Co}(\text{LN}_4)(\text{NO})]$  (**2**) at 50% thermal ellipsoids for all non-hydrogen atoms. Selected bond distances (Å) and angles (deg): (**1**) Fe1–N1, 1.9413(12); Fe1–N2, 1.9730(11); Fe1–N5, 1.700(12); N5–O1, 1.1705(14); Fe1–N5–O1, 153.23(10); (**2**) Co1–N1, 1.9277(10); Co1–N2, 1.9433(11); Co1–N5, 1.7890(11); N5–O1, 1.1551(15); Co1–N5–O1, 125.97(9).

The spectroscopic properties of **1** are typical of 5C Sq-Py  $\{\text{FeNO}\}^7$  species.<sup>12,14</sup> Complex **1** exhibits an  $S = \frac{1}{2}$  EPR signal with  $g_{\text{min}} = 2.02$  split into a triplet from hyperfine coupling to the  $I = 1$   $^{14}\text{N}$  nucleus of NO (toluene glass; 10 K; see the ESI†, Fig. S1). The FTIR spectrum exhibits one strong and single  $\nu_{\text{NO}}$  peak at 1704  $\text{cm}^{-1}$  (KBr matrix), which shifts to 1673  $\text{cm}^{-1}$  ( $\Delta\nu_{\text{NO}} = 31$   $\text{cm}^{-1}$ ) upon isotopic substitution with  $^{15}\text{NO}$  consistent with the harmonic oscillator model. More interestingly, **1** displays a reversible redox wave at  $E_{1/2} = -1.38$  V ( $\Delta E_p = 0.074$  V) vs.  $\text{Fc}/\text{Fc}^+$  in MeCN, which we assign to the  $\{\text{FeNO}\}^7 \rightleftharpoons \{\text{FeNO}\}^8$  couple (Fig. 2). In contrast, **2** displays a similar diffusion-controlled  $\{\text{CoNO}\}^8 \rightleftharpoons \{\text{CoNO}\}^9$  couple at  $-1.40$  V ( $\Delta E_p = 0.061$  V) vs.  $\text{Fc}/\text{Fc}^+$  in MeCN (see the ESI†). This similarity in  $E_{1/2}$  has been observed in isostructural Fe/Co-( $\text{N}_2\text{S}_2$ )NO systems suggesting that the frontier MOs of both MNO platforms in **1** and **2** are isoenergetic.<sup>15</sup> Reversible one-electron reductions have also been reported in the Fe-Por species,  $[\text{Fe}(\text{TPP})\text{NO}]^{6a-c}$  and  $[\text{Fe}(\text{OEP})\text{NO}]^{6a-c}$  as well as non-heme systems like  $[\text{Fe}(\text{cyclam})\text{NO}]$ .<sup>7</sup> Thus, at least on the electrochemical time scale, the  $\text{LN}_4$  imine/pyrrolide platform is capable of supporting coordinated and

reduced nitrogen oxide ligands. To further probe the nature of the Fe center in **1**, its Mössbauer spectrum was measured (see the ESI†, Fig. S27). The observed isomer shift ( $\delta$ ) of 0.11(3) mm/s for **1** is more consistent with  $\{\text{FeNO}\}^6$  rather than  $\{\text{FeNO}\}^7$  complexes suggesting  $\text{NO}^+$ -like character and a low-spin Fe(I) oxidation state. This assignment would support the near-linear Fe–N–O bond although theoretical studies suggest more of a resonance structure (*vide infra*).

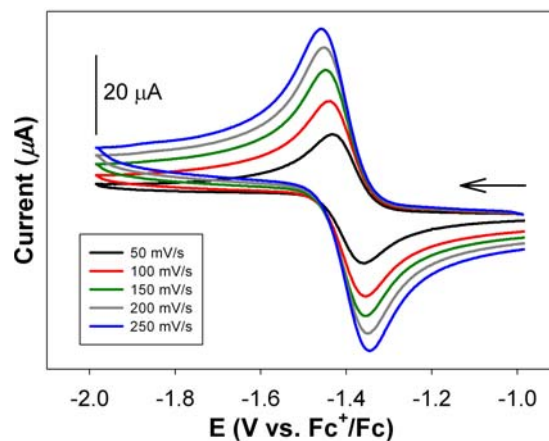


**Fig. 2** Cyclic voltammograms (CVs) of a 2 mM MeCN solution of  $[\text{Fe}(\text{LN}_4)(\text{NO})]$  (**1**) at different scan rates as indicated in the inset (0.1 M  $^n\text{Bu}_4\text{NPF}_6$  supporting electrolyte, glassy carbon working electrode, Pt-wire counter electrode, RT). Arrow displays direction of scan.

The electrochemical reversibility of **1** suggested that the corresponding  $\{\text{FeNO}\}^8$  complex should be isolable. When **1** was reacted under anaerobic conditions with one mol-equiv of dexamethylcobaltocene =  $[\text{Co}(\text{Cp}^*)_2]$  in toluene at RT, a violet solid formulated as the  $\{\text{FeNO}\}^8$  complex,  $[\text{Co}(\text{Cp}^*)_2][\text{Fe}(\text{LN}_4)(\text{NO})]$  (**3**), precipitated from the reaction mixture in quantitative yield (Scheme 1). In contrast to other reported  $\{\text{FeNO}\}^8$  complexes that have been generated *in situ* or at low temperature,<sup>6–8</sup> **3** was isolated as an air-sensitive solid at RT. The reduction was also found to be chemically reversible; treating an MeCN solution of **3** with ferrocenium salts like  $\text{FcPF}_6$  resulted in quantitative regeneration of **1**.

This  $\{\text{FeNO}\}^8$  complex (**3**) has been characterized by elemental microanalysis and several spectroscopic techniques. Additionally, its electronic structure was determined by DFT computations (*vide infra*). Complex **3** is soluble in polar organic solvents like MeCN forming dark violet-colored solutions where it exhibits good stability ( $t_{1/2} = 4.25$  h) in stark contrast to the few reported  $\{\text{FeNO}\}^8$  systems.<sup>6–8</sup> The ultimate fate of dissolved **3** appears to be a disproportionation reaction into **1** and an Fe(I)-dinitrogen complex via a transient dinitrosyl, which complicates the isolation of single crystals of **3**.<sup>16</sup> The UV-vis spectrum of **3** (MeCN, 298 K) exhibits two distinct visible bands at 560 nm ( $\epsilon: 1,810 \text{ M}^{-1} \text{ cm}^{-1}$ ) and 781 nm ( $\epsilon: 450 \text{ M}^{-1} \text{ cm}^{-1}$ ) with an intense  $\pi$ - $\pi^*$  band at 293 nm ( $53,000 \text{ M}^{-1} \text{ cm}^{-1}$ ) primarily due to the associated  $[\text{Co}(\text{Cp}^*)_2]^+$  counter-cation (Fig. 1 and the ESI†, Fig. S10). The intensity of the 560 nm band is suggestive of a charge-transfer electronic transition although the exact nature (i.e. ligand-metal or metal-ligand) has yet to be elucidated. Complex **3** is diamagnetic as exhibited by its  $^1\text{H}$  NMR spectrum in  $\text{CD}_3\text{CN}$ , implying an overall  $S = 0$  ground state at RT.  $^{15}\text{N}$  NMR of **3**

confirms this diamagnetism and reveals a single and downfield-shifted  $^{15}\text{N}$  resonance at 743 ppm (Fig. 3), a value at the upper limit for bent metal-nitrosyls.<sup>17</sup> The chemical shift of **3** is similar to the only  $\{\text{FeNO}\}^8$  complex with a reported  $^{15}\text{N}$  chemical shift ( $\delta = 790$  ppm in  $\text{CD}_2\text{Cl}_2$ ).<sup>6c</sup> The isoelectronic  $\{\text{CoNO}\}^8$  complex **2** (Co–N–O:  $126^\circ$ ) exhibits an  $^{15}\text{N}$  peak at 821 ppm (see the ESI†, Fig. S7), further supporting the bent nature of the Fe–N–O unit in **3**.

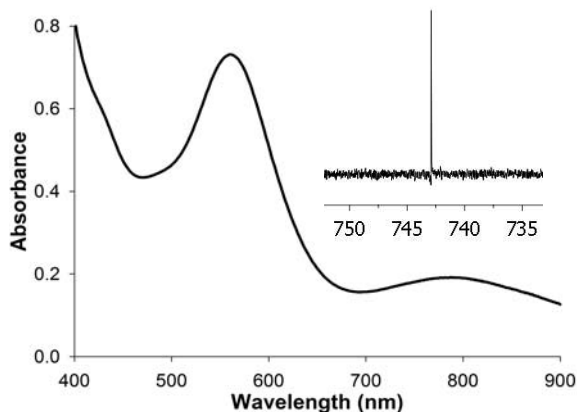


**Fig. 3** UV-vis spectrum of **3** (MeCN, 298 K). See the SI for the full spectrum displaying the  $\pi$ - $\pi^*$  transition of the  $[\text{Co}(\text{Cp}^*)_2]^+$  cation. Inset:  $^{15}\text{N}$  NMR of **3** ( $\text{CD}_3\text{CN}$ ,  $\text{CH}_3\text{NO}_2$  reference, 298 K).

Vibrational spectra of  $\{\text{FeNO}\}^8$  complexes have been difficult to interpret in Fe-Por systems due to overlap with ligand vibrations but have been observed in the  $1440$ – $1600$   $\text{cm}^{-1}$  range experimentally<sup>6</sup> and theoretically,<sup>18</sup> consistent with a mixed low-spin-Fe(II)- $\text{NO}^- \leftrightarrow$  low-spin-Fe(I)- $\text{NO}^\bullet$  description.<sup>18</sup> In contrast, the non-heme  $\{\text{FeNO}\}^8$  complex,  $[\text{Fe}(\text{cyclam-ac})\text{NO}]$ , displays a low-intensity  $\nu_{\text{NO}}$  peak at  $1271$   $\text{cm}^{-1}$  (generated *in situ* at  $-20$   $^\circ\text{C}$ ).<sup>7</sup> Complex **3** exhibits an intense  $\nu_{\text{NO}}$  band at  $1604$   $\text{cm}^{-1}$  that overlaps with ligand peaks and shifts to  $1570$   $\text{cm}^{-1}$  upon  $^{15}\text{NO}$  isotopic substitution ( $\Delta\nu_{\text{NO}} = 34$   $\text{cm}^{-1}$ ) suggesting more of a metal-centered reduction. The non-heme pyrrole-based  $\text{LN}_4$  complex is thus comparable to porphyrin  $\{\text{FeNO}\}^8$  systems. In support of this designation, DFT calculations by another group on a  $5\text{C } S = 0$  Fe-por  $\{\text{FeNO}\}^8$  system calculated  $\nu_{\text{NO}} = 1578$   $\text{cm}^{-1}$ .<sup>18b</sup> Despite the absence of a structure, high-resolution FTMS of **3** and **3- $^{15}\text{NO}$**  give rise to the expected parent ion peak in the negative ion mode ( $m/z = 312.0553$  for **3**;  $m/z = 313.0521$  for **3- $^{15}\text{NO}$** ) with the predicted isotopic distribution pattern (see the ESI†, Fig. S9), further supporting the  $\{\text{FeNO}\}^8$  formulation. The Mössbauer spectrum of **3** is consistent with Fe-NO unit reduction affording  $\delta = 0.51(3)$  mm/s ( $\Delta E_Q = 1.41(5)$  mm/s (Fig. 4)) and is comparable to the only other Mössbauer-characterized  $\{\text{FeNO}\}^8$  system by Wieghardt that displays  $\delta = 0.41$  mm/s.<sup>7</sup> This drastic increase in  $\delta$  from **1**-to-**3** ( $\Delta\delta = 0.40$  mm/s) indicates a change in the overall  $\pi$ -accepting ability of the ligand as a similar trend is observed in the isostructural  $[\text{Fe}(\text{cyclam-ac})\text{X}]^{n+/}$  series (where  $\text{X} = \text{NO}^+$ ,  $\text{NO}$ , and  $\text{NO}^-$ ). Thus, on reduction of **1**-to-**3** one would expect a decrease in the  $\pi$ -acid nature of the nitrosyl suggesting more  $\text{NO}^{\bullet/-}$  character in **3**. Taken together, complex **3** is the first example of a relatively stable and isolable  $\{\text{FeNO}\}^8$  complex that has been characterized by a variety of techniques in both the solution- and solid-state and at RT.

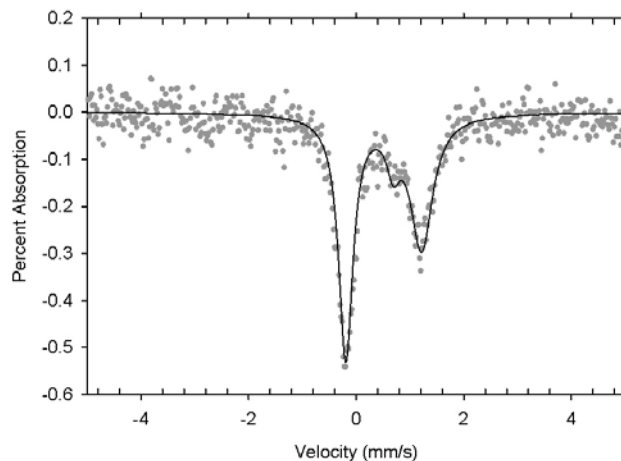


**Fig. 4** Zero-field Mössbauer spectrum of **3** recorded at 298 K. MB spectrum contains contributions from two separate Fe species accounting for 75 and 25% of the spectrum, which we assign as **3** and **1**, respectively. An additional  $\sim 10\%$  high-spin ferrous impurity has been removed from the original spectrum. The solid line shown is a least-square fit to the experimental data points of a simulated spectrum of the major Fe species with  $\delta = 0.51(3)$  mm/s and  $\Delta E_Q = 1.41(5)$  mm/s.

DFT (OLYP/STO-TZP; ADF 2009) calculations accurately reproduce the experimental geometries of **1** and **2**,<sup>19</sup> highlights of which are presented in the SI (see the ESI†, Table S3). The  $\{\text{FeNO}\}^7$  bending potential (see the ESI†, Fig. S25) is exceedingly soft and effectively barrierless,<sup>11c</sup> reflecting a superposition of multiple MO energies that rise or fall as the Fe–N–O unit bends away from linearity. It is therefore remarkable that our calculations reproduce the unusual pseudo-linear Fe–N–O angle of **1** with such accuracy.<sup>11d</sup> Perhaps even more intriguingly, these calculations predict additional examples of quasilinear  $\{\text{FeNO}\}^7$  units. This study, in a sense, represents the first practical realization of our predictions, whereas the other examples predicted remain to be experimentally realized. In contrast to the  $\{\text{FeNO}\}^7$  angle, the observed Co–N–O angle corresponds to a normal, steep-walled minimum.

The three key  $M(d)\text{--NO}(\pi^*)$  orbital interactions that define the bonding in these complexes are depicted in Fig. 5. The  $a''$ -symmetry  $d_{yz}$ -based MO is very similar in all  $\{\text{MNO}\}^{7/8}$  derivatives. However, defining the equatorial  $\text{N}_4$  plane as the  $xy$  plane, mixes the  $d_{xz}$  and  $d_{z2}$  orbitals somewhat in  $\{\text{FeNO}\}^7$  **1**. As a result, the  $d_{z2}$ -like orbital in **1** is distinctly tilted relative to the  $\text{N}_4$  plane. In other words, these two  $d$ -orbitals interact in an intermediate  $\sigma$ - $\pi$  manner with the  $\text{NO } \pi^*_x$  orbital, with the  $d_{z2}$ -like orbital more  $\sigma$  in nature. In the  $\{\text{Fe/CoNO}\}^8$  case, the  $d_{z2}$ -based orbital interacts in a more purely  $\sigma$  fashion with  $\text{NO } \pi^*_x$  (Fig. 5). M–NO  $\pi$ -bonding thus appears to be stronger for **1** than in **2**, consistent with the significantly shorter M–NO distance in the former. Careful examination of the MOs also indicates that the  $\pi$ -bonding in the  $\{\text{FeNO}\}^8$  case **3**, as measured by average  $\text{NO } \pi^*$  character in the  $\pi$ -bonding MOs, is intermediate between the  $\{\text{FeNO}\}^7$  and  $\{\text{CoNO}\}^8$  cases. Except for the  $d_{xy}$ -based orbital, which is purely nonbonding in all cases, the other  $d$ -based occupied MOs of **1-3** all have about 1/3 to 1/2  $d$ -character and a comparable proportion of  $\text{NO } \pi^*$  character. The M–NO bonding is thus invariably highly covalent and, as elsewhere, we would describe the electronic structure of  $\{\text{FeNO}\}^7$  **1** as halfway between low-spin-Fe(I)- $\text{NO}^+$  and low-spin-Fe(III)- $\text{NO}^-$ .<sup>11b,c,20</sup> In

general, the metal character of the MOs is somewhat higher in the Co case than in Fe, suggesting a Co(II)-NO• description; however, given the covalence, it might be better to describe as a resonance structure between low-spin-Co(II)-NO• ↔ low-spin-Co(III)-NO<sup>-</sup>. On going from {FeNO}<sup>7</sup> to {FeNO}<sup>8</sup>, the Mulliken charge (Table S4) decreases (in an algebraic sense) at Fe, the NO, and for a number of atoms on the equatorial ligand. The reduction in **3** is thus neither Fe- nor NO-centered but rather occurs over the entire FeNO group consistent with an electronic structure between low-spin-Fe(II)-NO<sup>-</sup> ↔ low-spin-Fe(I)-NO• (*vide supra*). Additional insights into the nature of {FeNO}<sup>8</sup> complex **3** were obtained from calculations of singlet-triplet (S-T) splittings and electron affinities (EAs). Thus, OLYP/TZP calculations indicated an S-T splitting of 0.6 eV for **3**, essentially identical to those of {CoNO}<sup>8</sup> complex **2** and of {FeNO}<sup>8</sup> and {CoNO}<sup>8</sup> porphyrin derivatives. Although hybrid functionals resulted in a small amount of broken-symmetry character (as evidenced by separation of  $\alpha$  and  $\beta$  spin densities) across the {MNO}<sup>8</sup> unit, there was no evidence for a non-innocent equatorial ligand with any method. The OLYP calculations further indicated similar EAs of about 1.4 eV for both **3** and for the analogous {FeNO}<sup>7</sup> porphyrin, suggesting that barring difficult solubility problems or the propensity for disproportionation, a variety of {FeNO}<sup>8</sup> derivatives should be isolable.

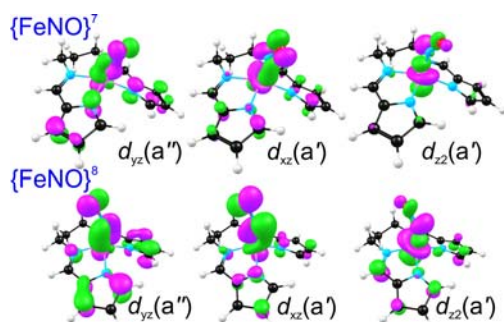


**Fig. 5** M(d)-NO( $\pi^*$ ) overlaps in the three HOMOs of optimized equilibrium structures of the experimental conformations of **1** and geometry-optimized low-energy conformation of **3** (ESI†, Table S3).

The reactions of {FeNO}<sup>8</sup> systems have yet to be explored and we have probed the reactivity of the {MNO}<sup>8</sup> complexes **2** and **3** in the present account. The most biologically significant and facile reaction of nitroxyl is with thiols<sup>1,3</sup> and heme proteins.<sup>3,21</sup> Moreover, NO/HNO preferentially targets Fe(III)-heme centers to form stable {FeNO}<sup>7</sup> species through reductive nitrosylation.<sup>1,3</sup> We thus tested the nitroxyl donor ability of {MNO}<sup>8</sup> systems **2** and **3** with established biological targets such as metMb. This technique is the standard and most sensitive method for characterizing HNO donors.<sup>22</sup> Reaction of equine skeletal metMb with the {MNO}<sup>8</sup> complex **3** in buffer (pH 7.2) resulted in immediate formation of MbNO in quantitative yield as monitored by UV-vis spectroscopy (Fig. 6). The metMb Soret band at 409 nm red-shifts to 422 nm immediately upon addition of **3** with the appearance of the double-humped Q-bands (540, 575 nm) that are characteristic of MbNO (Fig. 6). In contrast, the reductive nitrosylation of sperm whale metMb with Angeli's salt (Na<sub>2</sub>N<sub>2</sub>O<sub>3</sub>) takes 15.5 min to go to completion.<sup>22</sup> Since thiols have higher affinity for HNO than hemes,<sup>22</sup> we also performed a competition experiment with glutathione (GSH) in the metMb

reaction (see the ESI†, Fig. S16). Indeed, reaction of **3** with metMb under identical conditions in the presence of GSH completely inhibited reductive nitrosylation. Although classic HNO-donors react with thiols to form disulfide and hydroxylamine, it appears as if **3** reacts with GSH to form the reduced Roussin red ester (rRRE) compound, [Fe<sub>2</sub>( $\mu$ -GS)<sub>2</sub>(NO)<sub>4</sub>]<sup>-</sup>, as determined by UV-vis of the reaction medium in the absence of metMb.<sup>23</sup> The {FeNO}<sup>7</sup> complex **1** and {CoNO}<sup>8</sup> complex **2** do not react with metMb under identical conditions; however, **1** does nitrosylate ferrous Mb (deoxyMb), which suggests that **3** may reductively nitrosylate metMb in a two-step process *viz.* reduction of metMb following NO-transfer. The reactivity of **3** is similar to reported non-metal-based HNO donors and has not been explored with previously reported {FeNO}<sup>8</sup> complexes, possibly due to the unstable nature of these earlier systems. Although the exact nature of the NO ligand in **3** cannot be completely verified, these results do confirm the reduced character of the nitrogen oxide ligand in **3** and demonstrate that these species have the potential to be utilized as *quantitative nitroxyl-donors at ambient temperature and at physiological pH*.

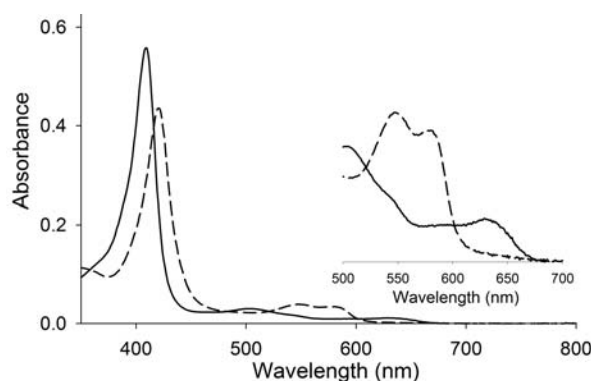


**Fig. 6.** UV-vis spectrum of a 2.97  $\mu$ M solution of metMb before (black line) and after (2 min mixing; black dashed line) reaction with **3** (5 mol-equiv) at 293 K in 50 mM phosphate buffer (pH 7.2). Inset: expansion of the Q-band region.

## Conclusions

In summary, we have described the synthesis and spectroscopic/structural/theoretical characterization of discrete {FeNO}<sup>7/8</sup> (**1** and **3**) and {CoNO}<sup>8</sup> (**2**) complexes. Complex **3** is a rare example of a thermally stable {FeNO}<sup>8</sup> complex isolated as a solid under ambient conditions.<sup>6c</sup> This work also presents the first insight into the electronic structure, spectroscopic features, reactivity, and potential fate of {FeNO}<sup>8</sup> units in biology. Furthermore, the reduced {FeNO}<sup>8</sup> complex **3** has proven as a useful reductive nitrosylation agent towards metMb under physiological conditions and demonstrates promise for these types of complexes as future HNO therapeutics. In fact, the endogenous production of nitroxyl has not yet been clearly established. Presumably, this is due to the short half-life ( $t_{1/2} = 2.5$  s), lack of detection methods, and the use of HNO-donors that produce other reactive nitrogen species or don't operate ideally at physiological pH.<sup>1</sup> The development of better donor systems is thus a current need that these complexes could meet.

## Acknowledgements

T.C.H. acknowledges the Department of Chemistry at the University of Georgia (UGA) for start-up funds and the UGA Research Foundation for a Faculty Research Grant. We wish to thank Prof. Jeff Urbauer and Prof. Michael K. Johnson for assistance and insightful discussions on the  $^{15}\text{N}$  NMR and EPR studies, respectively. G.C.P. thanks the NSF for support under Grant DMR-0604049. We also wish to thank Prof. I. Jonathan Amster and Mr. Franklin E. Leach III for assistance with the high-resolution MS studies and Dr. A. Viescas for assistance in fitting the MB spectra. The computational work was supported by a grant of supercomputer time from the Research Council of Norway (A.G.).

## Notes and references

<sup>a</sup>Department of Chemistry and Center for Metalloenzyme Studies, The University of Georgia, 1001 Cedar St, Athens, GA, USA. Fax: 706-542-9454; Tel: 706-542-3486; E-mail: tharrop@uga.edu

<sup>b</sup>Department of Physics, Villanova University, Villanova, PA, USA. Tel: 610-519-4883; E-mail: gpd@villanova.edu

<sup>c</sup>Department of Chemistry, University of the Free State, 9300 Bloemfontein, Republic of South Africa.

<sup>d</sup>Department of Chemistry and Center for Theoretical and Computational Chemistry, University of Tromsø, N-9037 Tromsø, Norway. Fax: 47-776-4476; Tel: 47-776-4407; E-mail: abhik@chem.uit.no

<sup>†</sup>Electronic Supplementary Information (ESI) available: synthesis and characterization data, details of the DFT computations, and CIF files. See DOI: 10.1039/b000000x/

- (a) J. M. Fukuto, A. S. Dutton, and K. N. Houk, *ChemBioChem*. 2005, **6**, 612-619; (b) N. Paolocci, M. I. Jackson, B. E. Lopez, K. Miranda, C. G. Tocchetti, D. A. Wink, A. J. Hobbs, and J. M. Fukuto, *Pharmacol. Ther.* 2007, **113**, 442-458; (c) J. C. Irvine, R. H. Ritchie, J. L. Favalaro, K. L. Andrews, R. E. Widdop, and B. K. Kemp-Harper, B. K. *Trends Pharmacol. Sci.* 2008, **29**, 601-608.
- (a) H. T. Nagasawa, S. P. Kawle, J. A. Elberling, E. G. DeMaster, and J. M. Fukuto, *J. Med. Chem.* 1995, **38**, 1865-1871; (b) D. A. Wink, K. M. Miranda, T. Katori, D. Mancardi, D. D. Thomas, L. Ridnour, M. G. Espey, M. Feelisch, C. A. Colton, J. M. Fukuto, P. Pagliaro, D. A. Kass, and N. Paolocci, *Am. J. Physiol.: Heart Circ. Physiol.* 2003, **285**, H2264-H2276; (c) N. Paolocci, T. Katori, H. C. Champion, M. E. St. John, K. M. Miranda, J. M. Fukuto, D. A. Wink, and D. A. Kass, *Proc. Natl. Acad. Sci. USA* 2003, **100**, 5537-5542; (d) K. M. Miranda, N. Paolocci, T. Katori, D. D. Thomas, E. Ford, M. D. Bartberger, M. G. Espey, D. A. Kass, M. Feelisch, J. M. Fukuto, and D. A. Wink, *Proc. Natl. Acad. Sci. USA* 2003, **100**, 9196-9201.
- (a) P. J. Farmer and F. Sulc, *J. Inorg. Biochem.* 2005, **99**, 166-184; (b) K. M. Miranda, *Coord. Chem. Rev.* 2005, **249**, 433-455; (c) J. A. Reisz, E. Bechtold, S. B. King, *Dalton Trans.* 2010, **39**, 5203-5212; (d) M. R. Kumar, J. M. Fukuto, K. M. Miranda, P. J. Farmer, *Inorg. Chem.* 2010, **49**, 6283-6292.
- (a) B. A. Averill, *Chem. Rev.* 1996, **96**, 2951-2964; (b) W. G. Zumft, *J. Inorg. Biochem.* 2005, **99**, 194-215; (c) A. Daiber, T. Nauser, N. Takaya, T. Kudo, P. Weber, C. Hultschig, H. Shoun, and V. Ullrich, *J. Inorg. Biochem.* 2002, **88**, 343-352.
- J. H. Enemark and R. D. Feltham, *Coord. Chem. Rev.* 1974, **13**, 339-406.
- (a) D. Lançon and K. M. Kadish, *J. Am. Chem. Soc.* 1983, **105**, 5610-5617; (b) I.-K. Choi, Y. Liu, D. W. Feng, K.-J. Paeng, and M. D. Ryan, *Inorg. Chem.* 1991, **30**, 1832-1839; (c) J. Pellegrino, S. E. Bari, D. E. Bikiel, and F. Doctorovich, *J. Am. Chem. Soc.* 2010, **132**, 989-995; (d) Z. Wei and M. D. Ryan, *Inorg. Chem.* 2010, **49**, 6948-6954.
- R. G. Serres, C. A. Grapperhaus, E. Bothe, E. Bill, T. Weyhermüller, F. Neese, and K. Wieghardt, *K. J. Am. Chem. Soc.* 2004, **126**, 5138-5153.
- A. C. Montenegro, V. T. Amorebieta, L. D. Slep, D. F. Martín, F. Roncaroli, D. H. Murgida, S. E. Bari, J. A. Olabe, *Angew. Chem. Int. Ed.* 2009, **48**, 4213-4216.
- A. M. Wright, G. Wu, and T. W. Hayton, *J. Am. Chem. Soc.* 2010, **132**, 14336-14337.
- MeCN solutions of **2** appear to react with excess  $\text{O}_2(\text{g})$  to form  $\text{Co-NO}_{2/3}$  complexes. The reaction occurs over the course of several hours indicative of its overall stability. Complex **1**, however, is indefinitely stable to  $\text{O}_2(\text{g})$  purge in the solid-state.
- Examples of linear  $\{\text{FeNO}\}^7$  complexes: (a) P. Berno, C. Floriani, A. Chiesi-Villa, and C. Guastini, *J. Chem. Soc., Dalton Trans.* 1988, 1409-1412; (b) J. Conradie, D. A. Quarless Jr., H.-F. Hsu, T. C. Harrop, S. J. Lippard, S. A. Koch, and A. Ghosh, *J. Am. Chem. Soc.* 2007, **129**, 10446-10456; (c) J. Conradie, K. H. Hopmann, and A. Ghosh, *J. Phys. Chem. B* 2010, **114**, 8517-8524; (d) J. Conradie and A. Ghosh, *Inorg. Chem.* 2011, **50**, 4223-4225.
- (a) J. A. McCleverty, *Chem. Rev.* 2004, **104**, 403-418; (b) G. R. A. Wyllie and W. R. Scheidt, *Chem. Rev.* 2002, **102**, 1067-1089; (c) G. B. Richter-Addo and P. Legzdins, *Metal Nitrosyls*; Oxford University Press: New York, 1992.
- 5C Sq-Py  $\{\text{CoNO}\}^8$  complexes: (a) K. J. Franz, L. H. Doerrer, B. Spingler, and S. J. Lippard, *Inorg. Chem.* 2001, **40**, 3774-3780; (b) C.-Y. Chiang, J. Lee, C. Dalrymple, M. C. Sarahan, J. H. Reibenspies, and M. Y. Darensbourg, *Inorg. Chem.* 2005, **44**, 9007-9016. (c) G. B. Richter-Addo, S. J. Hodge, G.-B. Yi, M. A. Khan, T. Ma, E. Van Caemelbecke, N. Guo, and K. M. Kadish, *Inorg. Chem.* 1996, **35**, 6530-6538.
- L. E. Goodrich, F. Paulat, V. K. K. Praneeth, and N. Lehnert, *Inorg. Chem.* 2010, **49**, 6293-6316.
- C.-Y. Chiang, J. Lee, C. Dalrymple, M. C. Sarahan, J. H. Reibenspies, and M. Y. Darensbourg, *Inorg. Chem.* 2005, **44**, 9007-9016.
- The visible bands in the UV-vis spectrum of **3** (MeCN, 298 K) slowly decrease over 13 h (see the ESI<sup>†</sup>, Fig. S11) affording **1** and an Fe(I) species that we tentatively assign as  $[\text{Fe}(\text{LN}_4)\text{N}_2]^+$  based on the  $\nu_{\text{N}_2}$  band observed in the IR at  $\sim 2100\text{ cm}^{-1}$  (Fig. S13) and consistent with other Fe-N<sub>2</sub> species, see J. L. Crossland and D. A. Tyler, *Coord. Chem. Rev.* 2010, **254**, 1883 and references therein. This band also remains unshifted if you start with **3-<sup>15</sup>N**O (Fig. S13) whereas the  $\nu_{\text{NO}}$  of the formed **1** does shift. The decay in these bands does not appear to change with solvent as a similar result is observed in THF at 298 K (data not shown). Disproportionation of  $\{\text{FeNO}\}^8$  species have also been reported with an *in situ* isolated  $\{\text{FeNO}\}^8$   $\beta$ -diketiminato species, see Z. J. Tonzetich, F. Héroguel, L. H. Do, and S. J. Lippard, *S. J. Inorg. Chem.* 2011, **50**, 1570.
- J. Mason, L. F. Larkworthy, and E. A. Moore, *Chem. Rev.* 2002, **102**, 913-934.
- (a) N. Lehnert, V. K. K. Praneeth, and F. Paulat, *J. Comput. Chem.* 2006, **27**, 1338-1351; (b) D. P. Linder and K. R. Rodgers, *Inorg. Chem.* 2005, **44**, 8259-8264.
- (a) A. Ghosh, K. H. Hopmann, and J. Conradie, *J. Inorg. Chem. Phys. Chem.* 2005, **177**, 1-10; (b) A. Ghosh, *Acc. Chem. Res.* 2005, **38**, 943-954.
- For an  $\text{NO}^+$  or  $\text{NO}^-$  description, the implication is that the electron density around NO is cylindrically symmetric. For an  $\text{NO}^\bullet$  description, however, one may be tempted to conclude that one of the NO  $\pi^*$  orbitals will carry an unpaired electron. This is not observed. The unpaired spin density on NO is cylindrically symmetric and is distributed roughly evenly between the two  $\pi^*$  orbitals. This is why we describe the situation as halfway between  $\text{NO}^+$  or  $\text{NO}^-$ . However, since the description is anyway a shorthand for the detailed MO picture, people may choose to describe the complex as  $\text{Fe(II)-NO}^\bullet$ , depending on their taste.
- L. J. Ignarro, *Nitric Oxide Biology and Pathobiology*; Academic Press: San Diego, 2000.
- (a) D. A. Bazylinski and T. C. Hollocher, *J. Am. Chem. Soc.* 1985, **107**, 7982-7986; (b) M. P. Doyle, S. N. Mahapatro, R. D. Broene, and J. K. Guy, *J. Am. Chem. Soc.* 1988, **110**, 593-599; (c) D. Andrei, D. J. Salmon, S. Donzelli, A. Wahab, J. R. Klose, M. L. Citro, J. E. Saavedra, D. A. Wink, K. M. Miranda, and L. Keefer, *J. Am. Chem. Soc.* 2010, **132**, 16526-16532.
- The UV-vis of a buffered (pH 7.2) solution containing GSH and **3** results in distinct low-energy absorption bands at  $\sim 650$  and  $980\text{ nm}$  characteristic of rRRE compounds. For examples see Z. J. Tonzetich, H. Wang, D. Mitra, C. E. Tinberg, L. H. Do, F. E. Jenney Jr., M. W. W. Adams, S. P. Cramer, and S. J. Lippard, *S. J. J. Am. Chem. Soc.* 2010, **132**, 6914.